Ni and Ru Loading on $Sr_2Ta_2O_7$ by Electroless to Enhance Its Photocatalytic Hydrogen Evolution from Water

C.L Compean-González[1], V. M. Arredondo-Torres[2], M.E Zarazúa-Morin[1], M.Z Figueroa-Torres[1*]

[1]Departamento de Ecomateriales y Energía, Facultad de Ingeniería Civil, Universidad Autónoma de Nuevo León, Av. Universidad s/n Ciudad Universitaria San Nicolás de los Garza Nuevo León, México. CP. 66451.
[2]Facultad de Químico Farmacobiología, Universidad Michoacana de San Nicolás de Hidalgo, Tzintzuntzan #173, Col. Matamoros, Morelia, Michoacán, México. C.P. 58240
*Tel: +5214424400 ext. 5106; e-mail: m_zyzlila@yahoo.com.mx

ABSTRACT

Water splitting using a photocatalyst is one of the most attractive alternatives for hydrogen production. However, most semiconductors cannot give high H_2 evolution activities without a cocatalyst even in the presence of sacrificial electron donors. This work evaluates the effect of the surface modification with nickel and ruthenium on the hydrogen evolution of strontium tantalate. X-ray powder diffraction results shows that the single phase of $Sr_2Ta_2O_7$ was obtained at 900 ℃. The optical energy band gab was calculated from UV-vis absorption sprectrum and Kubelka-Muck formula giving a Eg value of 4.6 eV. Specific surface areas was estimated by nitrogen adsorption at -196 °C and the BET equation, the material exhibited a surface area of 3.58 m^2/g. Nickel and ruthenium loading on $Sr_2Ta_2O_7$ surface was done by using electroless deposition technique at 40 and 70 ºC respectively. By scanning electron microscopy it was observed that the particle size of $Sr_2Ta_2O_7$ was around 0.5 μm and the Ni and Ru nanoparticles were highly dispersed onto its surface with a narrow size range between 5-15 nm. It was found that hydrogen evolution under UV irradiation was increased when a suitable amount of nanoparticles is dispersed. Moreover, the higher hydrogen evolution was achieved when Ni was used as cocatalysts, increasing 1.4 times the hydrogen production compared with the pure $Sr_2Ta_2O_7$.

Keywords: electroless; UV-light, cocatalyst

1. Introduction

Hydrogen has been recognized as an important energy carrier, especially for use it in fuel cells, environmentally friendly vehicles, domestic heating, and stationary power generation. Clean and sustainable hydrogen production is still a challenge for scientists to solve energy and environmental problems. Photocatalytic water splitting using a semiconductor material is one of the most promising technologies for producing hydrogen; this is because H_2 can be obtained directly from water and solar light radiation, both of which are abundant and renewable resources [1,2].

Since Fujishima and Honda first demonstrated the photocatalytic water splitting on TiO_2 electrode, extensive efforts have been made to improve the reaction efficiency using metal oxide semiconductors [3,4]. Many metal oxides, such as titanates ($SrTiO_3$, BaTiO), niobates ($K_4Nb_6O_{17}$, $Ba_5Nb_4O_{15}$) and tantalates ($NaTaO_3$, $LaLnTa_2O_7$) have been developed as photocatalysts material for water splitting. Among these material, the oxides with layered crystal structures exhibited attractive photocatalytic activity for water splitting due to their interlayer acts as reaction sites [5–7]. Several research groups have proposed that metals ions with electronic d^{10} configuration improve charge separation and transport which enhance photocatalytic water splitting [4,8]. However, most semiconductors cannot give high H_2 evolution activities without a cocatalyst even in the presence of sacrificial electron donor. As it is known, loading a cocatalyst on the surface of semiconductor is often indispensable for achieving efficient hydrogen evolution [9,10]. The Sr_2TaO_7 with a perovskite-layered structure showed photocatalytic activity for hydrogen evolution from water [11]. In the literature, it is stated that water splitting is enhanced by the addition of nickel oxide onto its surface. They prove that hydrogen gas is formed on the nickel oxide surface and the oxygen is released from the photocatalyst surface [12]. On the other hand, the actuals methods for loading cocatalysts on a semiconductor surface are not efficient enough because of the dispersion of nanoparticles is low and it is hard to control the particle size and shape. In this sense, the search of alternative low-cost and short preparation time techniques to highly disperse nanoparticles are desirable. The electroless plating method is an attractive alternative and suitable choice for nanoparticles deposition because it has been proved to control the loading amount, particle size and dispersion [13]. In the present study $Sr_2Ta_2O_7$ were synthesized by solid-state reaction method and the influence Ni and Ru cocatalysts loading by using electroless deposition on the photocatalytic activity of Sr_2TaO_7 for hydrogen evolution were investigated.

2. Experimental

2.1. Preparation of $Sr_2Ta_2O_7$

The $Sr_2Ta_2O_7$ compound was prepared by a conventional solid-state reaction method. $SrCO_3$ (Sigma-Aldrich 99.9%) and Ta_2O_5 (Sigma-Aldrich 99.9%) were used as raw materials. The powders were dried at 200 ºC for 4 h before the synthesis. Then, stoichiometric amounts of each reactant were mixed with acetone in an agate mortar until the acetone completely evaporated. The solid mixture was placed into a platinum crucible and calcined between 800 and 1000 °C under an air atmosphere using a heating rate of 5 °C min^{-1} for 24 h with intermediate regrinding to complete the reaction.

2.2. Nickel and Ruthenium loading on $Sr_2Ta_2O_7$ surface

Fist, the $Sr_2Ta_2O_7$ surface was activated by the conventional two-step $SnCl_2/PdCl_2$ procedure [14]. The conditions of the nickel electroless deposition (ED) were taken from the work of Figueroa-Torres et. al. [15] and for ruthenium deposition from the work of Cheng-Hong et al. [16]. The ED deposition was carried out by adding the $Sr_2Ta_2O_7$ on a baker with electroless solution. Then the solution was placed on a hot plate at the desired temperature with a magnetic stirrer. Deposition temperatures were from 30 to 80 °C. The amount of nickel and ruthenium loading were controlled by deposition time. After electroless treatment, the Ni/ $Sr_2Ta_2O_7$ and Ru/ $Sr_2Ta_2O_7$ samples were separated from the solution by filtration, rinsed several times with distilled water and dried at 80 °C.

2.3. Characterization

$Sr_2Ta_2O_7$ samples were characterized by X-ray powder diffraction (XRD) using Cu Kα radiation as the incident X-ray source. XRD data were collected at room temperature from 10° to 70° with a step interval of 0.01° and a counting time of 1 s $step^{-1}$. Morphologies of samples were observed by scanning electron microscope (SEM) adapted with energy dispersive spectrometry system (EDS) which was used to determine the amount of Ni and Ru deposited. To evaluate the surface area of the samples, physical adsorption of N_2 at – 196 °C was carried out. Before measurements, samples were outgassed at 300 °C for 3 h. Surface area (A_{BET}) was obtained using the multipoint BET method. Optical absorption properties of the samples were analyzed in the range of 200–900 nm at room temperature with a UV–vis spectrophotometer with an integrating sphere attachment. Optical Energy band gap (Eg) values were obtained using the Kubelka–Munk function based on the diffuse reflection (DR UV–vis) spectra data.

2.4. Photocatalytic Hydrogen Production Evaluation

The photocatalytic water splitting reaction was carried out at low pressure in a reactor with inner quartz cell and a 400 W high pressure mercury lamp as the irradiation source. Firstly, 0.3 g of the materials was dispersed into 300 mL of pure water under vigorous stirred. Prior to the reaction, argon was bubbled to deaerate the solution. Pressure was set at 100 Torr and temperature was kept at 20 °C using a cooling system. The evolved gases were analyzed using a chromatograph equipped with a TCD detector and column Hayesep D 100/120 using argon as carrier gas. Reaction evolution was analysed each 30 min during 4 h.

3. Results and discussion

Figure 1 shows the XRD diffractograms of $Sr_2Ta_2O_7$ synthesized by solid-state reaction method at different temperatures. The diffractograms of the raw materials indicated that they are pure because only Sr_2CO_3 and Ta_2O_7 phases were presented. According to XRD analysis results, at 800 °C, $Sr_2Ta_2O_7$ phase begins to crystallize, it is observed a diffractogram with wide diffraction peaks that can be identified like a mixture of phases of the corresponding raw oxides and the first diffraction peaks of $Sr_2Ta_2O_7$. As temperature increased to 900 °C, the $Sr_2Ta_2O_7$ phase was only identified. As can be seen, the diffraction

peaks were intensive and narrow, suggesting a good crystallization degree. The further increase in the temperature do not generate significant changes in the diffractograms.

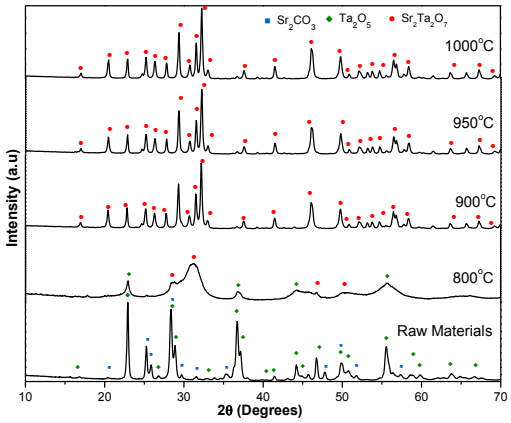

Fig 1. XRD patterns of $Sr_2Ta_2O_7$ prepared by solid-state reaction at different temperatures.

Figure 2 shows SEM images of $Sr_2Ta_2O_7$. In figure 2a, it can be observed big agglomerates of particles with sizes of more than 15 μm. This can be attributed that solid state reaction occurs at 900 °C favoring the partial sintering of particles. At higher magnifications (Fig 2b) it is possible to observe that the agglomerates are formed by $Sr_2Ta_2O_7$ particles of semispherical shape with a smooth surface. The average particle size is round 300 nm.

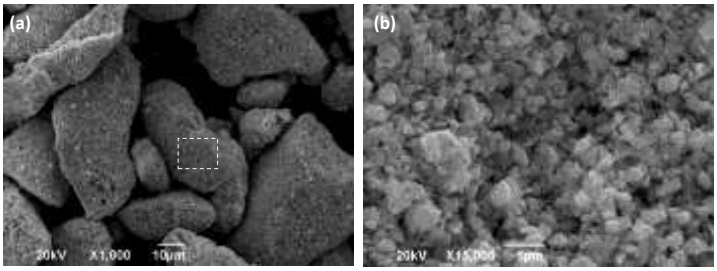

Fig 2. SEM images of $Sr_2Ta_2O_7$ prepared by solid-state reaction.

In order to find convenient deposition parameters to disperse Ni or Ru on $Sr_2Ta_2O_7$ surface, different temperature and deposition time were tested. Figure 3 shows weight percent of Ni or Ru deposited at different temperatures as function of deposition time. From the figure 3, it can be appreciated that temperature was an important factor that influences Ni and Ru deposition process. Particularly, the Ni deposition can be done from ambient temperature (30°C) or higher temperatures. At 30 and 40 °C, the

reaction rate allows a good control of the deposited Ni nanoparticles amount as function of time. However, an increase from 40 to 50 °C the deposition rate was highly increased; in a few minutes, the Ni deposited amount is twice. On the other hand, it was found that for Ru deposition required higher temperatures to deposition reaction started. Below 70 °C the reaction did not initiate even at long deposition time. Between 70 and 80 °C the reaction rate is appropriate to control the Ru loading amount.

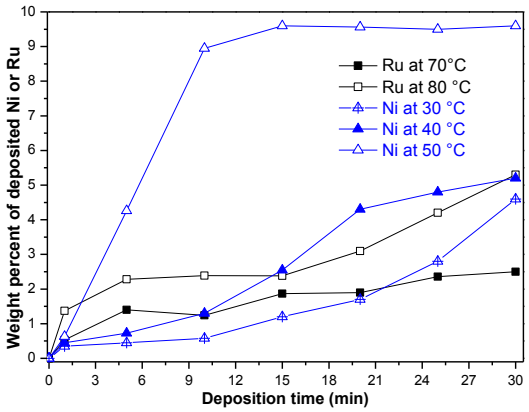

Fig 3. Weight percent of Ni or Ru as function of deposition time at different temperatures on $Sr_2Ta_2O_7$.

The morphology of the Ni and Ru on the $Sr_2Ta_2O_7$ surface is illustrated in figure 4. The image reveals that Ni and Ru nanoparticles are uniformly dispersed through the $Sr_2Ta_2O_7$ surface. Moreover, presented a semispherical shape with a narrow size range between 5 to 15 nm. The EDS spectrum confirms the presence of Ni and Ru nanoparticles.

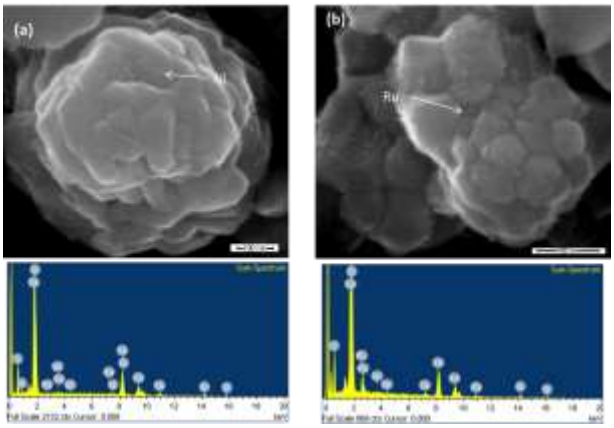

Fig 4. SEM images and EDS spectrum of Ni and Ru nanoparticles on $Sr_2Ta_2O_7$.

The optical absorption properties of $Sr_2Ta_2O_7$ and 1 %wt. $Ni/Sr_2Ta_2O_7$ and 1%wt. $Ru/ Sr_2Ta_2O_7$ were measured by UV-Vis spectroscopy, and the results are shown in figure 5. As can be seen from the figure, the $Sr_2Ta_2O_7$ shows a very weak absorption at the visible range region. It is evident that the loading on Ni and Ru nanoparticles promotes the absorption of light in the visible region. The optical band gap values obtained by using the Kubelka–Munk function and extrapolating the linear portion against photoenergy are reported in table 1.

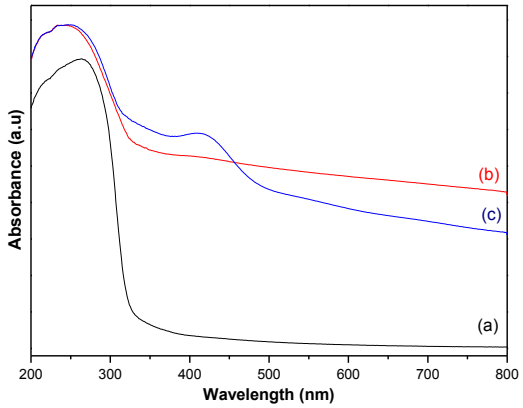

Fig. 5. UV–vis absorbance spectra of (a) $Sr_2Ta_2O_7$; (b) $1\%Ni/ Sr_2Ta_2O_7$ and (c) $1\%Ru/ Sr_2Ta_2O_7$.

The Eg values were 4.6 eV. This property is not modified by the loading of nanoparticles because of they are on the oxide surface. Table 1 also reports the specific surface area values. The $Sr_2Ta_2O_7$ exhibit a surface area of 3.58 m^2/g. After electroless deposition, the surface area was increased more than twice; this is mainly due to $Sr_2Ta_2O_7$ particles deagglomerated during electroless deposition; this is and additional benefic that can have a favorable influence in the photocatalytic activity of the material. It is also appreciated that the increase in surface area was independent of the metal type and metal amount.

Table 1. Optical band-gap and surface area values

Sample	**Eg (eV)**	**A_{BET} (m^2/g)**	
		Before ED	**After ED**
$Sr_2Ta_2O_7$			N/A
$Ni/Sr_2Ta_2O_7$	4.6	3.58	9.9
$Ru/Sr_2Ta_2O_7$			9.5

Prior to the photocatalytic reaction test, blank controls were performed with the same reaction system in dark or in the absence of photocatalyst. No hydrogen was generated under these conditions, thus the hydrogen production is due to the presence of the photocatalyst material. Figure 6a illustrate the photocatalytic hydrogen evolution as a function of irradiation time from pure water of Ni/$Sr_2Ta_2O_7$ samples and the hydrogen evolution of Ru/$Sr_2Ta_2O_7$ are presented in figure 6b. According to the results showed in Figure 6, it was observed that $Sr_2Ta_2O_7$ is able to produce hydrogen without loading a cocatalyst. However, the loading metals provide efficient active sites for H_2 evolution. It can be seen that during the 30 first minutes, samples presented a similar behavior after that time; differences were found in the hydrogen evolution as function of the metal type and metal loading amount. It can be seen that exits a better synergism when Ni is used as cocatalysts than Ru. It was found that for nickel between 0.15 and 1 wt % is an appropriate amount to enhance hydrogen evolution. At higher contents, hydrogen evolution decreased and it is even less than $Sr_2Ta_2O_7$ alone. For the ruthenium samples, the enhance in hydrogen production is not significant and higher amounts of Ru are required compared to Ni-samples. The better H_2 production was achieved with the sample with 2 wt% of Ru.

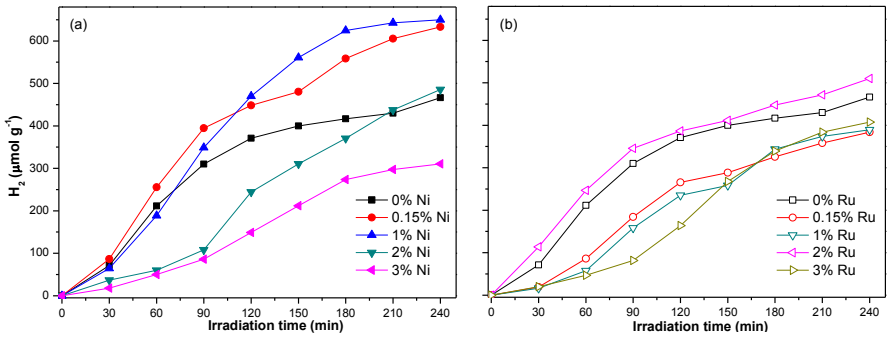

Fig. 6. Photocatalytic hydrogen production a) Ni/$Sr_2Ta_2O_7$ and b) Ru/$Sr_2Ta_2O_7$ samples

The H_2 evolution rate of the samples is reported in table 2. The H_2 evolution of 0.15 wt.%Ni/ $Sr_2Ta_2O_7$ was 158 μm/h g, which is approximately 1.4 times higher that of $Sr_2Ta_2O_7$. Whilst for the 2wt.%Ru/ $Sr_2Ta_2O_7$ sample was 128 μm/h g, which is 1.1μm/h g times higher than $Sr_2Ta_2O_7$. When and overload of metal was used, the decrease in H_2 evolution can be associated with a limited light absorption by $Sr_2Ta_2O_7$, which reduces the generation of electron-hole pairs and they also can acts as recombination centers.

Table 2. Hydrogen evolution rates

	H_2 evolution rate ($\mu m\ h^{-1}\ g^{-1}$)	
Metal wt.%	**Ni**	**Ru**
0	116	116
0.15	158	95
1	162	98
2	121	128
3	77	102

4. Summary and perspectives

This work demonstrates that electroless deposition technique is an attractive alternative route to highly dispersed Ni and Ru nanoparticles of approximately 5 to 15 nm in a few minutes on $Sr_2Ta_2O_7$ surface. Ni and Ru nanoparticles are effective cocatalysts to enhance hydrogen evolution reaction. However, exist a better synergism when Ni is used in an appropriated amount. The highest hydrogen evolution was presented by 1wt% Ni/ $Sr_2Ta_2O_7$ sample. At this Ni content, hydrogen amount was 1.4 times higher than $Sr_2Ta_2O_7$.

Acknowledgements

Presented work was supported by the CONACYT thought the project CB-2012-177079 and PROMEP/103.5/13/6644 projects and in part by projects PAICYT-UANL-IT881-11 and FOTOSÍNTESIS ARTIFICIAL 75/2012.

References

[1] K. Maeda, Photocatalytic water splitting using semiconductor particles: History and recent developments. J. Photochem. Photobiol. C Photochem. Rev. 2011; 12: 237–268.
[2] D. Jing, L. Guo, L. Zhao, X. Zhang, H. Liu, M. Li, S. Shen, G. Liu, X. Hu, and X. Zhang, Efficient solar hydrogen production by photocatalytic water splitting: From fundamental study to pilot demonstration. Int. J. Hydrogen Energy. 2010; 35: 7087–7097.
[3] A. Ibhadon and P. Fitzpatrick, Heterogeneous Photocatalysis: Recent Advances and Applications. Catalysts, 2013; 3: 189–218.
[4] H. Kisch, Semiconductor photocatalysis: mechanistic and synthetic aspects, Angew. Chem. Int. Ed. Engl. 2013; 52: 812–847.
[5] Y. Inoue, Photocatalysts with tunnel structures for decomposition of water, J. Chem. Soc. Faraday Trans. 2010; 90: 797–802.
[6] Y. Miseki and A. Kudo, Water splitting over new niobate photocatalysts with tungsten-bronze-type structure and effect of transition metal-doping, ChemSusChem 2011; 4: 245–251.
[7] H. Xu, R. Q. Zhang, A. M. C. Ng, A. B. Djuri, H. T. Chan, W. K. Chan, and S. Y. Tong, Splitting Water on Metal Oxide Surfaces, 2011; 115: 19710–19715.
[8] Y. Inoue, Photocatalytic water splitting by RuO_2 loaded metal oxides and nitrides with d^0 and d^{10} related electronic configurations, 2009; 2: 364–386.
[9] J. Yang, D. Wang, H. Han, and C. A. N. Li, Roles of Cocatalysts in Photocatalysis and Photoelectrocatalysis, 2013; 46: 1900-1909.

[10] M. Tian, W. Shangguan, J. Yuan, S. Wang, and Z. Ouyang, Promotion effect of nanosized Pt , RuO_2 and NiO_x loading on visible light-driven photocatalysts $K_4Ce_2M_{10}O_{30}$ (M = Ta , Nb) for hydrogen evolution from water decomposition, Sci. Tech. Adv. Mat. 2007: 8: 82-88.

[11] C. Zhou, G. Chen, Y. Li, H. Zhang, and J. Pei, Photocatalytic activities of $Sr_2Ta_2O_7$ nanosheets synthesized by a hydrothermal method, 2009; 34: 2113–2120.

[12] A. Kudo, Photocatalyst materials for water splitting, 2003; 7:1–3.

[13] Z. Wu, S. Ge, M. Zhang, W. Li, and K. Tao, Journal of Colloid and Interface Science Synthesis of nickel nanoparticles supported on metal oxides using electroless plating: Controlling the dispersion and size of nickel nanoparticles, J. Colloid Interface Sci. 2009; 330: 359–366.

[14] T. N. Khoperia, Electroless deposition in nanotechnology and ULSI, 2003; 69: 384–390.

[15] M. Z. Figueroa-Torres, C. Domínguez-Ríos, J. G. Cabañas-Moreno, O. Vega-Becerra, and a. Aguilar-Elguézabal, The synthesis of Ni-activated carbon nanocomposites via electroless deposition without a surface pretreatment as potential hydrogen storage materials, Int. J. Hydrogen Energy 2012; 37: 10743–10749.

[16] C.-H. Liu, B.-H. Chen, C.-L. Hsueh, J.-R. Ku, M.-S. Jeng, and F. Tsau, Hydrogen generation from hydrolysis of sodium borohydride using Ni–Ru nanocomposite as catalysts, Int. J. Hydrogen Energy. 2009; 34: 2153–2163.